RSC Advances

PAPER

View Article Online
View Journal | View Issue

Cite this: *RSC Adv.*, 2020, **10**, 19371

MoS_4^{2-} intercalated NiFeTi LDH as an efficient and selective adsorbent for elimination of heavy metals

Garima Rathee,[a] Sahil Kohli,[a] Amardeep Awasthi,[a] Nidhi Singh[a] and Ramesh Chandra *[ab]

Received 26th March 2020
Accepted 10th May 2020

DOI: 10.1039/d0ra02766a

rsc.li/rsc-advances

The enormous increase of heavy metal pollution has led to a rise in demand for synthesizing efficient and stable adsorbents for its treatment. Therefore, we have designed a novel adsorbent by introducing $(MoS_4)^{2-}$ moieties within the layers of NiFeTi LDH-NO_3, *via* an ion exchange mechanism, as a stable and efficient adsorbent to deal with the increasing water pollution due to heavy metals. Characterization techniques such as XRD, FTIR, TGA, SEM, TEM, and Raman spectroscopy were used to confirm the formation of $(MoS_4)^{2-}$ intercalated NiFeTi LDH and structural changes after the adsorption process. The efficiency of the material was tested with six heavy metal ions, among which it was found to be effective for toxic Pb^{2+} and Ag^{+} ions. When selectivity was studied with all six of the metal ions copresent in one solution, the material showed greater selectivity for Pb^{2+} and Ag^{+} ions with the selectivity order of $Ni^{2+} < Cu^{2+} < Zn^{2+} < Fe^{3+} < Pb^{2+} < Ag^{+}$, with great adsorption capacities of 653 mg g^{-1} for Pb^{2+} and 856 mg g^{-1} for Ag^{+} metal ions. Further, the kinetics adsorption study for both the metal ions had a great correlation with the pseudo-second-order model and supported the chemisorption process *via* the formation of M–S bonding. The adsorption process obeyed the Langmuir model. Therefore, the MoS_4-LDH material could be a promising adsorbent for the removal of heavy metals.

1. Introduction

According to a recent survey by the GOES organization, water pollution is considered to be one of the leading environmental problems and could be a threat to existence of life on the planet in the upcoming decades.[1] Therefore, it has become a significant concern for various societies.[2] Direct emission of an enormous number of pollutants (such as dyes, pharmaceutical compounds, organic compounds, heavy metals, *etc.*) into water resources is the main root of water contamination.[3,4] Among the listed pollutants, pollution caused by heavy metals has become a fundamental environmental issue in environmental remediation and separation science due to its harmful effects on human health and the ecological environment.[5]

Heavy metals are considered to be those metals in chemistry that have higher atomic weight, atomic number, and a density greater than 5 g cm^{-3}.[6] They are further classified as toxic, precious, and radioactive metals.[7] Heavy metals with characteristics of non-biodegradability, carcinogenicity and mutagenesis, accumulate in the food chain and subsequently harm the human beings and other living bodies.[8] They are basically discarded by various industrial activities, for instance, electronics plating, metal finishing, textiles, metallurgy, mining, battery manufacturing, tanning, and chemical manufacturing.[9] Among all heavy metals, lead (Pb), mercury (Hg), chromium (Cr), cadmium (Cd), arsenic (As), zinc (Zn), copper (Cu), tin (Sn), nickel (Ni), silver (Ag) and cobalt (Co) are the most toxic ones.[10] However, heavy metals such as zinc and copper are also essential elements when present at lower concentrations but harmful when present at higher levels. Among the listed toxic metals, lead (Pb) is ranked as the second most hazardous element, and lead poisoning directly affects the liver, kidney, gastrointestinal system, and central nervous system.[11] Moreover, direct or indirect long-term lead exposure may cause hepatitis, anemia, nephritic syndrome, encephalopathy, brain damage, brain swelling, and also death.[12] Lead poisoning also causes mental disabilities and behavioral fluctuations, mainly in children and nearly 143 000 deaths annually in developing countries.[13] As a result, it has become imperative to eliminate such hazardous metal ions from wastewater before its disposal to water bodies.

Numerous methods such as ion exchange, electrical coagulation, flotation, bio-sorption, flocculation treatment, chemical precipitation, filtration membrane, and adsorption have been used worldwide for heavy metals removal and recovery from wastewater.[14–21] Among these treatment methods, adsorption is considered to be more promising because of its strong operability, low cost, and simple design.[22] Several synthetic and natural adsorbents such as activated carbon, zeolites, biomaterials, sorption resins, and polymers have been brought in the

[a]*Drug Discovery & Development Laboratory, Department of Chemistry, University of Delhi, Delhi-110007, India. E-mail: acbrdu@hotmail.com*

[b]*Dr B. R. Ambedkar Centre for Biomedical Research, University of Delhi, Delhi-110007, India*

application for efficient removal of heavy metals.[19–30] Clays with characteristics of high surface area, low cost, and hydrophilicity have gained attraction as natural adsorbents for heavy metal ions treatment.

Layered double hydroxides (LDHs), a type of anionic clays, comprises of positively charged layers intercalated with counter anions. The outstanding intercalated anion exchange properties of LDHs allow it to show multipurpose applications in the field of 2-D nanoreactors, catalysts, scavengers, and adsorbents.[31–36] Also, sulfides are known to form strong heavy metals-sulfides covalent bonds, which can be very beneficial in designing new efficient adsorbent materials for heavy metal capture from heavy metals contaminated wastewater.[37,38] With the attractive applications of LDHs and sulfide containing groups, we can assume that after functionalizing LDHs with the sulfide containing groups, a single-phase having the advantages of both the materials (oxides and sulfides) would be acquired with enriched properties of heavy metals contaminated wastewater remediation. Previously, Ma and coworkers[42] have fabricated a novel adsorbent for the removal of heavy metals by intercalating MoS_4^{2-} ions in binary MgAl LDH, and the same was characterized by using various techniques confirming the intercalation of MoS_4^{2-} ions in the layers of binary MgAl LDH. They employed the same for the uptake of heavy metals for wastewater.[42]

Our research group has previously fabricated a ternary NiFeTi LDH and applied it for the elimination of various anionic dyes from wastewater.[39] Herein, we have designed a novel modified LDH form by functionalizing ternary NiFeTi LDH with $(MoS_4)^{2-}$ ions in the interlayers and investigated its ability of heavy metal removal from the wastewater system. The ascribed MoS_4-intercalated LDH material exhibits excellent adsorption ability for Pb^{2+} and Ag^{+} at a fast rate as compared to previously used binary LDH moieties for such uptakes. Therefore, the ability to reduce heavy metal concentrations below <5 ppb levels makes MoS_4-LDH a good alternative for wastewater remediation in the future.

2. Experimental section

2.1 Materials

NiFeTi–CO_3 LDH was reproduced using a previously reported hydrothermal method.[39] NiFeTi–CO_3 LDH was further converted into NiFeTi–NO_3 LDH by using the ion-exchange method.[40] Ammonium tetrathiomolybdate ($(NH_4)_2MoS_4$) was obtained from SigmaAldrich. Also, NO_3^- anion from NiFeTi–NO_3 LDH was replaced by $(MoS_4)^{2-}$ anion to acquire brown colored MoS_4-LDH. For $(MoS_4)^{2-}$ anion exchange, 0.3 g NiFeTi–NO_3 LDH and 0.3 g $(NH_4)_2MoS_4$ were dispersed and further stirred for 36 hours in 20 mL of deionized water at ambient temperature. The obtained solid was filtered, also washed with degassed water, and then with acetone. The resulting material was air-dried to get brown colored MoS_4-LDH.

2.2 Uptake of heavy metals

The uptake studies of heavy metals from aqueous solutions at various concentrations were carried out using the batch method. At the initial stage, heavy metal uptake experiments were carried for six metal ions (Ag^+, Pb^{2+}, Zn^{2+}, Fe^{3+}, Cu^{2+}, and Ni^{2+}) coming from their corresponding nitrate salts. The solid adsorbent was dispersed in metal ion solutions for a fixed duration of time, followed by centrifugation to separate the solid sorbent, and finally, the metal ion concentrations were determined from their respective supernatant solutions by using atomic absorption spectroscopy (AAS). The difference in the metal concentrations of mother solutions and supernatant solutions was used to evaluate the adsorption capacity. The distribution coefficient (K_d) is estimated by using the given equation:

$$K_d = (V[(C_0 - C_f)/C_f])/m \quad (1)$$

where C_0 represents initial concentrations of respective M^{n+} ion (ppm), C_f denotes the final concentrations of respective M^{n+} ion (ppm) after contact, m represents the amount of solid adsorbent in g and V stands for volume of the solution used for adsorption process.[41] The heavy metal removal% is determined by

$$\%\ \text{Removal} = 100 \times (C_0 - C_f)/C_0 \quad (2)$$

The removal capacity of adsorbent (q_m) is obtained by

$$q_m = ((C_0 - C_f)V/m) \times 10^{-3} \quad (3)$$

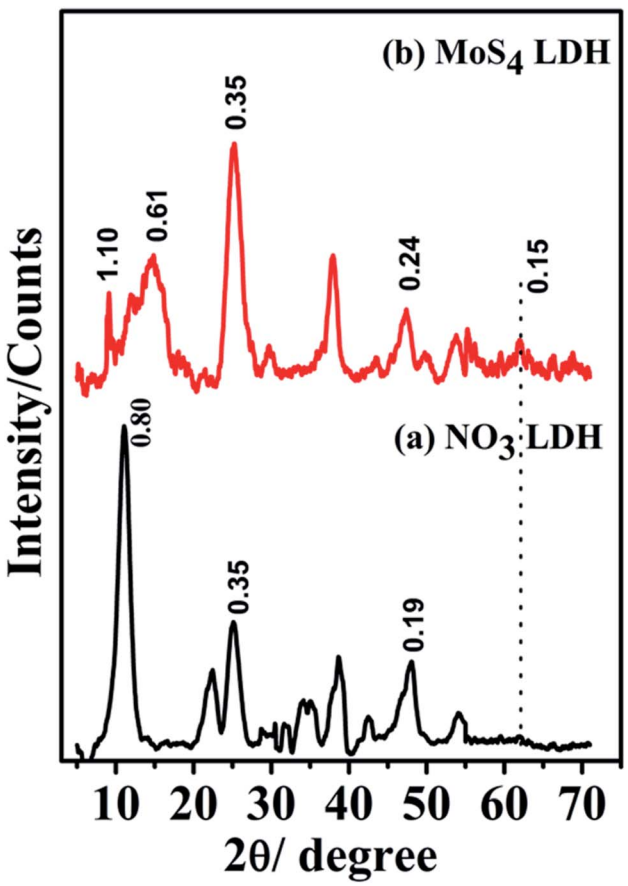

Fig. 1 XRD patterns of (a) NO_3 LDH and (b) MoS_4 LDH.

The adsorption studies for the heavy metals (except for Ag) were carried out at v/m ratio = 3846 mL g^{-1} and for Ag at 8333 mL g^{-1} because when batch experiments were employed for Ag at v/m ratio of 3846 mL g^{-1}, the efficiency of synthesized material for the uptake of Ag ions was very much fast and showed 100% uptake efficiency within 5 min of experiment and became difficult to evaluate the kinetic study. Further, the high selectivity for Ag^{+} and Pb^{2+} was determined by using a mixture of all the metal ions together with ~100 ppm initial concentration for each ion. Experiments were also carried out to examine the removal capacity (q_m) for Ag^{+} and Pb^{2+} by varying the initial metal ion concentrations at ambient temperature for a contact time of 2 hours. The acquired data was used for determining the adsorption isotherms.

2.3 Kinetics study

Adsorption kinetic study was performed for Ag^{+} and Pb^{2+} ions at different adsorption times (5–120 min). For the kinetic study of Ag^{+} ion, 0.006 g of sorbent was dispersed in 50 mL of 100 ppm Ag solution with a v/m ratio of 8333 mL g^{-1}. After fixed time intervals, suspensions were drawn out, centrifuged, and ion content was analyzed using AAS. Similar kinetic experiment was performed for Pb^{2+} with 0.013 g of sorbent for 50 mL of 100 ppm Pb^{2+} solution (v/m = 3846 mL g^{-1}).

2.4 Characterization techniques

The XRD patterns of synthesized materials were collected using an X-ray diffractometer (Model no. D8 DISCOVER). Fourier transformed infrared (FT-IR) spectra were recorded on IRAffinity-1S FTIR Shimadzu. Morphology was determined by JEOL JSM 6610 SEM with an accelerating voltage of 30 kV and by TECNAI 200 kV HRTEM (Fei, Electron Optics). BET specific surface area of LDH was determined using Autosorb iQ Station 1, Quantachrome Instruments by Brunauer–Emmett–Teller (BET) method. The metal ion concentrations were determined using ZEEnit 700 Atom Absorption Spectrometer.

3. Results and discussion

3.1 Characterization of synthesized MoS_4-LDH

The obtained brown colored MoS_4 LDH was characterized thoroughly using various characterization techniques such as XRD, FTIR, SEM, TEM, BET, Raman, and TGA.

The XRD patterns of NO_3 LDH and the ion-exchanged product MoS_4 LDH is depicted in Fig. 1. The comparison of

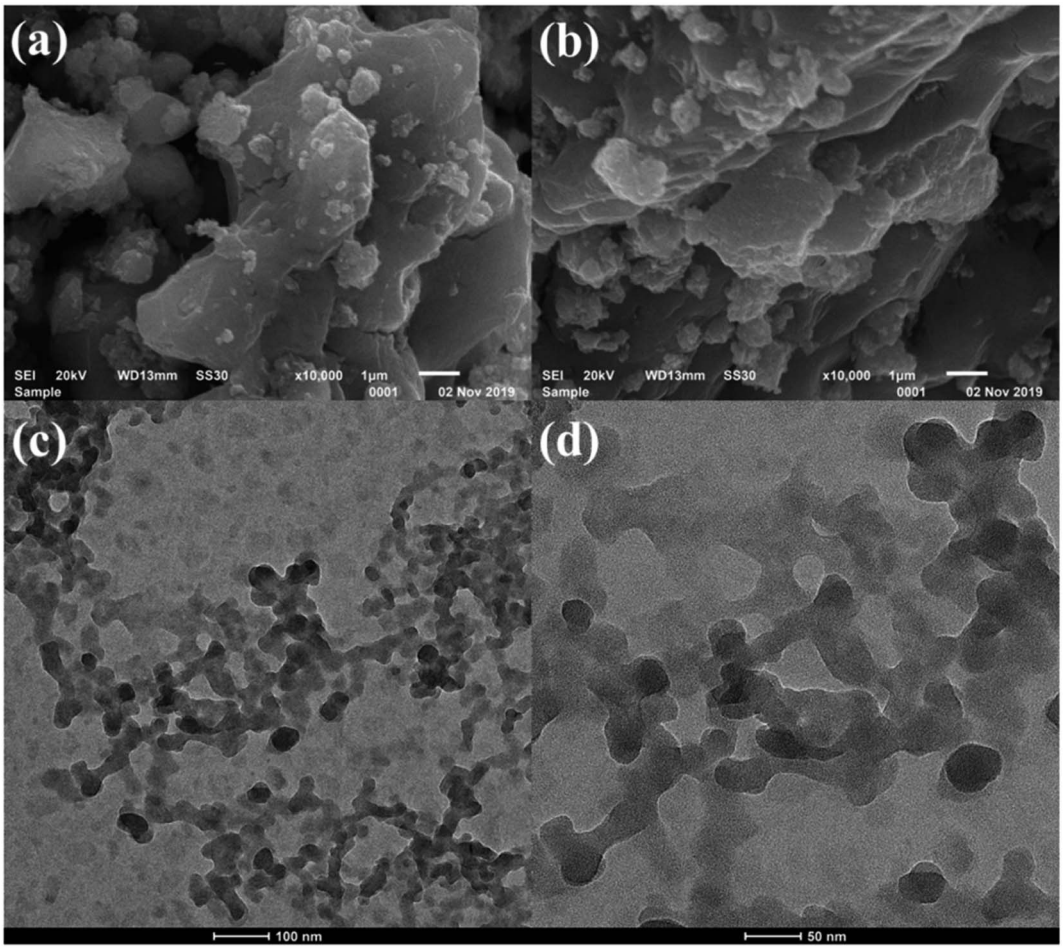

Fig. 2 SEM (a and b) and TEM (c and d) images of MoS_4 LDH.

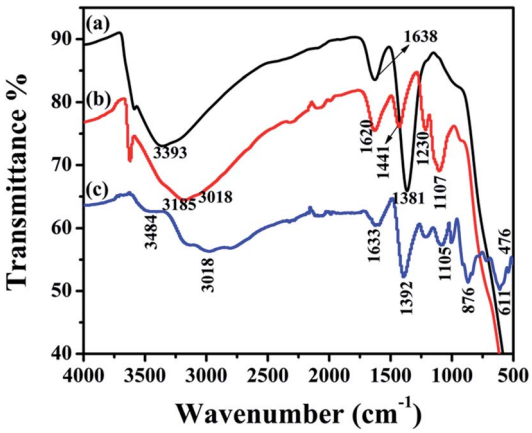

Fig. 3 FTIR spectra of (a) NO_3-LDH and (b) MoS_4-LDH and (c) $(NH_4)_2MoS_4$.

basal spacing of NO_3 LDH (d_{basal} = 0.80 nm) (Fig. 1a) with the enlarged MoS_4 LDH spacing (d_{basal} = 1.10 nm) (Fig. 1b), confirms the exchange of NO_3-ions with MoS_4-ions in the interlayer spacing of LDH. The layered phase is approved by the existence of (00*l*) reflections at 1.10, 0.61 and 0.35 nm. The lower intensity of (003) reflection at 1.10 nm as compared to that of (006) reflection at 0.61 nm could be attributed to the heavy nature and substantial scattering property of MoS_4-ions intercalated in the layers of LDH.[42,51]

SEM and HRTEM images are depicted in Fig. 2. SEM images illustrate the layered structures of MoS_4^{2-} intercalated NiFeTi LDH. SEM images clearly show that the layered structure of MoS_4 LDH resembles the CO_3-LDH, as reported in our previous work.[39]

The intercalation of MoS_4-ions *via* the exchange of NO_3^- ions from interlayers is confirmed by FTIR analysis. Fig. 3a illustrates the spectrum of NO_3-LDH, which confirms the formation of NO_3^- intercalated LDH. Strong band appearing at 1381 cm^{-1} could be attributed to the stretching vibration of nitrate ion in the layers of LDH. A broad band at 3393 cm^{-1} is assigned to the stretching vibration occurring because of the O–H group of interlayered water molecules and metal bonded hydroxyl groups. The existence of a weaker band at 1638 cm^{-1} could be assigned to the O–H bending vibration of interlayered hydroxyl and water molecules. Fig. 3b illustrates the FTIR spectrum of MoS_4 LDH. The complete disappearance of NO_3^- band at 1381 cm^{-1} confirms the entire exchange of NO_3^- ions by MoS_4^{2-} ions. In the case of free $(NH_4)_2MoS_4$ (Fig. 3c), the appearance of the band at 476 cm^{-1} is allotted to the Mo–S vibration. The band at 3018 cm^{-1} could be assigned to the N–H mode of ammonium group (NH_4^+). The absorption band at 3484 cm^{-1} could have corresponded to the hydroxyl stretching vibration (O–H) of water molecules. The bands existing at 1392 and 1633 cm^{-1} might be attributed to the in-plane N–H bending mode.[39,42,43]

The thermal gravimetric analysis (TGA) is depicted in Fig. 4a. The initial weight loss at temperature range 100–150 °C is attributed to the elimination of interlayered water molecules (approximately 10% weight loss). The subsequent degradation till 330 °C is assigned to the partial loss of MoS_4^{2-} from MoS_4 LDH (31.57% weight loss). The complete elimination of MoS_4^{2-} from MoS_4 LDH occur up to 600 °C (weight loss (water molecules + MoS_4 ions) = 42.31%).[44]

Fig. 4b illustrates the N_2 adsorption–desorption isotherm carried out to study the porosity of MoS_4 LDH. From the BJH data, the surface area was found to be 64.66 m^2 g^{-1}. The pore volume and pore diameter were found to be 0.122 cm^3 g^{-1} and 3.832 nm, respectively. The isotherm type confirms the formation of mesopores.

Raman spectra of designed material and pure NH_4MoS_4 are depicted in Fig. 5. The Raman spectra were found to be very much helpful in studying the details of stretching bands due to Mo–S bonds. The pure form of NH_4MoS_4 clearly showed two peaks at 455 and 476 cm^{-1}, due to the Mo–S bond stretching. Whereas, the interaction of the intercalated MoS_4^{2-} with the hydroxides of LDH *via* hydrogen bonding results into a redshift due to which the bands occurs at 361 and 387 cm^{-1}.[42]

From all the shreds of evidence obtained from various characterizations, it could be stated that the NO_3-LDH was successfully converted into more negatively charged MoS_4-LDH.

3.2 Heavy metal uptake using MoS_4 LDH

The removal of heavy metals from aqueous solution by MoS_4-LDH adsorbent was examined using batch method

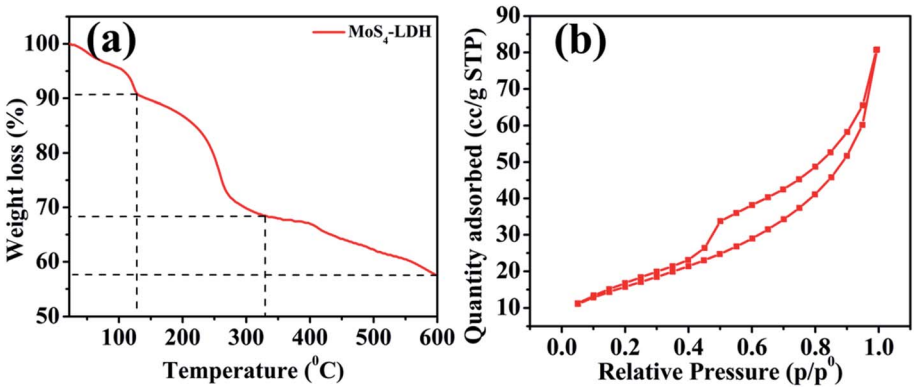

Fig. 4 TGA (a) and BET (b) spectra of MoS_4-LDH.

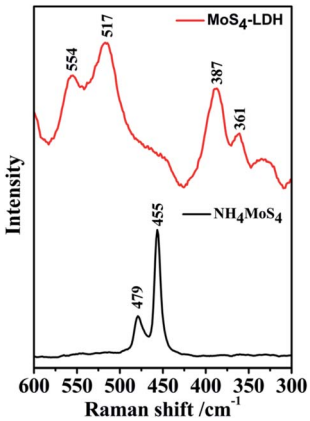

Fig. 5 Raman spectra of MoS_4-LDH.

experiments. The MoS_4-LDH affinity towards employed heavy metals was evaluated in the form of a distribution coefficient (K_d). The adsorption study was carried out using individual heavy metal solutions such as Ag^+, Pb^{2+}, Zn^{2+}, Fe^{3+}, Cu^{2+}, and Ni^{2+} and mixture solution containing all the six ions together. The obtained adsorption results for individual ions studies are illustrated in Table 1. From the results, it could be stated that MoS_4-LDH showed a greater ability for Ag^+ and Pb^{2+} as compared to other ions. Both the metal ions were removed entirely from 100 ppm metal ion concentrated solution with K_d values higher than 10^5. In contrast, MoS_4-LDH showed low adsorption capacity for other heavy metals, which makes it one of a suitable method for the elimination of such ions.

Table 2 illustrates the competitive adsorption results with all six ions in one solution. From the results, the selectivity order was obtained to be $Ni^{2+} < Cu^{2+} < Zn^{2+} < Fe^{3+} < Pb^{2+} < Ag^+$, and it can be stated that MoS_4-LDH showed high selectivity for soft Lewis acid metal ions. As compared to the results obtained from individual ions removal tests, Pb^{2+} and Ag^+ were found to be in high correlation, except for other ions. Hence, it can be said that ascribed material can rapidly eliminate heavy metals by reducing the concentration of soft Lewis heavy metals from aqueous solution by trapping the heavy metal ion *via* M–S coordination bond formation. All the results point out towards great potential of designed MoS_4-LDH as an efficient adsorbent for purifying heavy metals polluted water.

Adsorbent amount variation study was also evaluated for both metal ions (Ag^+ and Pb^{2+}), and results are depicted in Fig. 6a. From the study, it could be clearly stated that for the elimination of Pb^{2+} pollutants from wastewater, 0.0026 g of adsorbent was sufficient for complete removal of Pb^{2+} from 100 ppm sample and for Ag^+ removal 0.0012 g of MoS_4-LDH was appropriate for complete elimination from 100 ppm sample.

Further, the pH variation was also evaluated for Pb^{2+} and Ag^+ (varying from 4 to 8) by using 0.1 N HCl and 0.1 N NaOH solutions. Interestingly, it was found that no significant change in the

Table 1 Adsorption results toward individual ions[a]

Entry	Single ions	Initial conc. (ppm)	Final conc. (ppm)	M^{n+} removal (%)	K_d (mL g^{-1})
1	Pb^{2+}	100	0.4392	99.56	8.7×10^5
2	Zn^{2+}	100	17.25	82.75	1.8×10^4
3	Ni^{2+}	100	42.74	57.26	5.2×10^3
4	Fe^{3+}	100	29.49	70.51	9.2×10^3
5[b]	Ag^+	100	0.001	100	8.3×10^9
6	Cu^{2+}	100	74.08	25	1.3×10^3

[a] Ion concentration 100 ppm per ion (approx.), contact time = 90 min, V = 10 mL, m (mass of solid sample) = 0.0026 g, v/m ratio = 3846 mL g^{-1}. [b] m (mass of solid sample) = 0.0012 g, v/m ratio = 8333 mL g^{-1}.

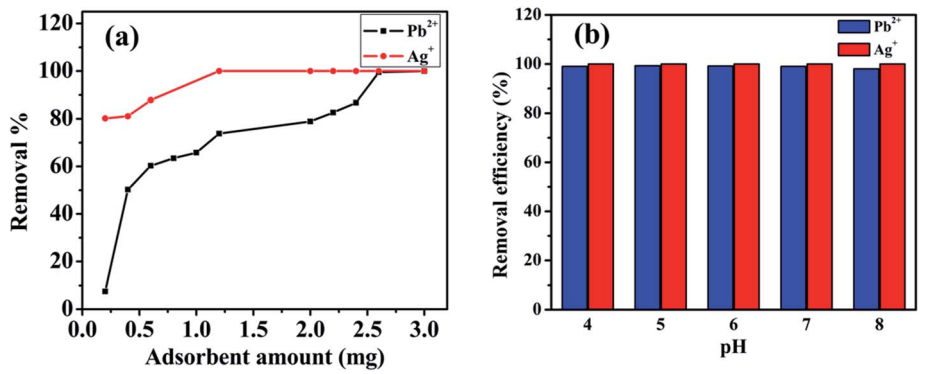

Fig. 6 (a) Adsorbent amount variation study for Pb^{2+} and Ag^+ removal, (b) effect of pH on removal efficiency.

Table 2 Adsorption results toward mixed ions[a]

Entry	Mixed ions	Initial conc. (ppm)	Final conc. (ppm)	M^{n+} removal (%)	K_d (mL g^{-1})
1	Pb^{2+}	128.9	4.7	96.35	1.01×10^5
2	Zn^{2+}	108.36	87.18	19.54	934.40
3	Ni^{2+}	83.66	76.5	8.55	359.97
4	Fe^{3+}	85.97	55.76	35.14	2.08×10^3
5	Ag^{+}	128.1	3.358	97.37	1.40×10^5
6	Cu^{2+}	98.5	82.725	16.015	733.43

[a] Ion concentration ~ 100 ppm per ion (approx.), contact time = 90 min, V = 50 mL, m (mass of solid sample) = 0.013 g, v/m ratio = 3846 mL g^{-1}.

removal efficiency was observed for both the cases (Pb^{2+} and Ag^{+}) when pH of the solution was varied from 4 to 8 (Fig. 6b).

3.3 Kinetic study

The adsorption kinetic study was examined for heavy metal ions, which are depicted in Fig. 7 (for Pb^{2+} and Ag^{+}) to determine the adsorption rate and its pathway towards equilibrium. The sorption rates for the elimination of Pb^{2+} and Ag^{+} from respective individual solutions were found to be very fast, as depicted in Fig. 7a. MoS_4-LDH efficiently removed >90% of Pb^{2+} within 5 min and 98% of Ag^{+} within 40 min. The adsorption equilibrium was attained within 80 min for all the employed heavy metals pollutants. The adsorption rate was estimated with the help of two different kinetic rate equations: pseudo-first-order and pseudo-second-order kinetics rate equations which can be defined as:

$$\text{Pseudo-first-order}: \log(q_e - q_t) = \log(q_e) - \frac{k_1}{2.303} t \quad (4)$$

$$\text{Pseudo-second-order}: \frac{t}{q_t} = \frac{1}{k_2 q_e^2} + \frac{1}{q_e} t \quad (5)$$

where q_e (mg g^{-1}) represents the amount of heavy metal adsorbed at equilibrium stage, q_t (mg g^{-1}) is the amount of heavy metal adsorbed at time t, k_1 (min^{-1}) is the rate constant for pseudo-first-order kinetic rate equation, k_2 (g mg^{-1} min^{-1}) denotes the rate constant for the pseudo-second-order kinetic equation. The values of k_1 and k_2 were obtained by linear plots: $\ln(q_e - q_t)$ *vs.* t and t/q_t against t, respectively. The kinetic parameters obtained from the linear kinetic plots for Pb^{2+} and Ag^{+} are summarized in Table 3. The pseudo-first-order linear plots are depicted in Fig. 7b and c, and the pseudo-second-order linear kinetic plots for adsorption of Pb^{2+} and Ag^{+} are depicted in Fig. 7e and f. From the kinetic plots of the metal ions, it could be easily stated that the adsorption process follows the pseudo-second-order rate equation and the correlation coefficient (R^2) is close to one, which suggests that the process involved is chemisorption.[42,50] The kinetic data displays that the adsorption of Ag^{+} ions attained the equilibrium faster than Pb^{2+} ions.

3.4 Adsorption isotherm study

Selective studies clearly illustrated that the MoS_4-LDH was highly efficient for the removal of Ag^{+} and Pb^{2+}. Further, the adsorption isotherm study was used to estimate the maximum sorption capacity of MoS_4 LDH for Ag^{+} and Pb^{2+}. From the studies, it was witnessed that Ag^{+} and Pb^{2+} capture by MoS_4 LDH increased successively when the concentration was increased (50–500 ppm). The percentage of heavy metals removed as a function of the concentration of Ag^{+} and Pb^{2+} is depicted in Fig. 8a and b. From the obtained results, the ascribed material effectively captured Ag^{+} and Pb^{2+} over a broad

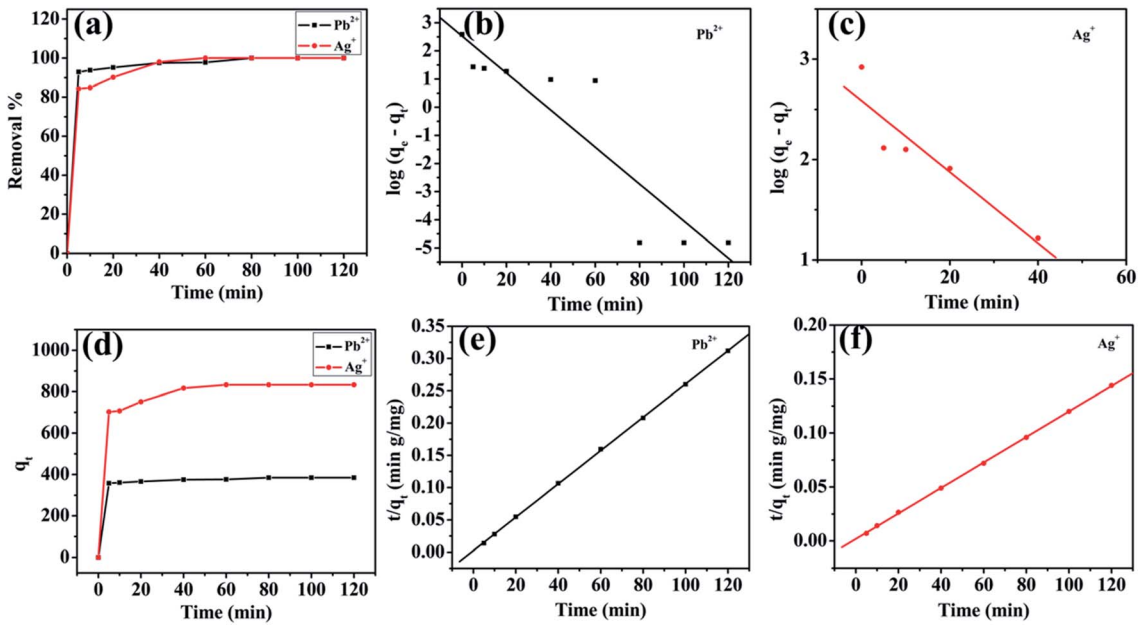

Fig. 7 Kinetics plots for Pb^{2+} and Ag^{+} removal: (a) contact time effect on removal%, (b) pseudo-first order plot for Pb^{2+} removal, (c) pseudo-first order plot for Ag^{+} removal, (d) adsorption capacity (q_t) as a function of time, (e) pseudo-second order plot for Pb^{2+} removal, (f) pseudo-second order plot for Ag^{+} removal.

Table 3 Kinetic parameters toward individual ions adsorption (Pb^{2+} and Ag^{+}) over MoS_4-LDH

	Pseudo-first order			Pseudo-second order			
Adsorbate	q_e (mg g^{-1})	k_1 (min^{-1})	R^2	q_e (mg g^{-1})	k_2 (g mg^{-1} min^{-1})	R^2	Calculated q_e (mg g^{-1})
Pb^{2+}	337.427	0.151	0.91	387.59	2.7×10^{-3}	0.999	385.23
Ag^{+}	385.363	0.0817	0.92	847.48	7.2×10^{-4}	0.999	839.16

range of concentrations. The maximum removal capacity (q_m) reached 856 and 653 mg g^{-1} for Ag^{+} and Pb^{2+}, respectively which is extraordinarily higher than the finest adsorbents for Ag^{+} removal such as magnetic cellulose xanthate (166 mg g^{-1}),[42] S_4-LDH (383 mg g^{-1})[46] and Mg/Al–MoS_4-LDH (450 mg g^{-1}).[42] Similarly, the obtained q_m value for Pb^{2+} is exceptionally higher than the previously reported adsorbents employed for the uptake of lead ion from contaminated water such as Mg/Al–MoS_4-LDH (290 mg g^{-1}),[42] DTPA-LDH (170 mg g^{-1})[47] and MNP–CTS (140 mg g^{-1}).[48] The comparison of the obtained q_m values of the ascribed material is depicted in Table 4.[42,45–49] From the comparison table, it can be stated that the synthesized MoS_4-LDH illustrates excellent elimination capacities for heavy metal ions, which could be attributed to the intercalation of MoS_4^{2-} in the gallery of NiFeTi-LDH.

Langmuir isotherm model was also used to evaluate the data in which adsorbate is assumed to form monolayer coverage on the surface of the adsorbent, and once such coverage is formed, no further sorption could occur at that active site. The Langmuir isotherm is defined by the following equation:

$$\frac{C_e}{q_e} = \frac{1}{q_m b} + \frac{C_e}{q_m} \quad (6)$$

where q_e (mg g^{-1}) denotes adsorption capacity after achieving equilibrium, q_m (mg g^{-1}) represents theoretical maximum adsorption capacity, C_e (mg L^{-1}) denotes heavy metal ion equilibrium concentration, and b (L mg^{-1}) is the Langmuir constant. The equilibrium adsorption capacity as a function of equilibrium concentrations for both the ions are depicted in Fig. 8c and d. Also, the Langmuir isotherms are depicted in Fig. 8e and f. The data for both the heavy metal ions were found to be in great correlation with the Langmuir model and theoretically obtained q_m values (848 (mg g^{-1}) for Ag^{+} and 653 (mg g^{-1}) for Pb^{2+}) are approximately equal to the obtained experimental values. The Langmuir parameters are summarized in Table 5. Correlation coefficient approaching unity ($R^2 > 0.99$) shows a linearly well-fitted curve with the Langmuir model, which confirms the monolayer adsorption and no occurrence of transmigration in the adsorbates.[44]

Further, the Freundlich isotherm model is also evaluated. In general, this model is based on the assumption that the non-

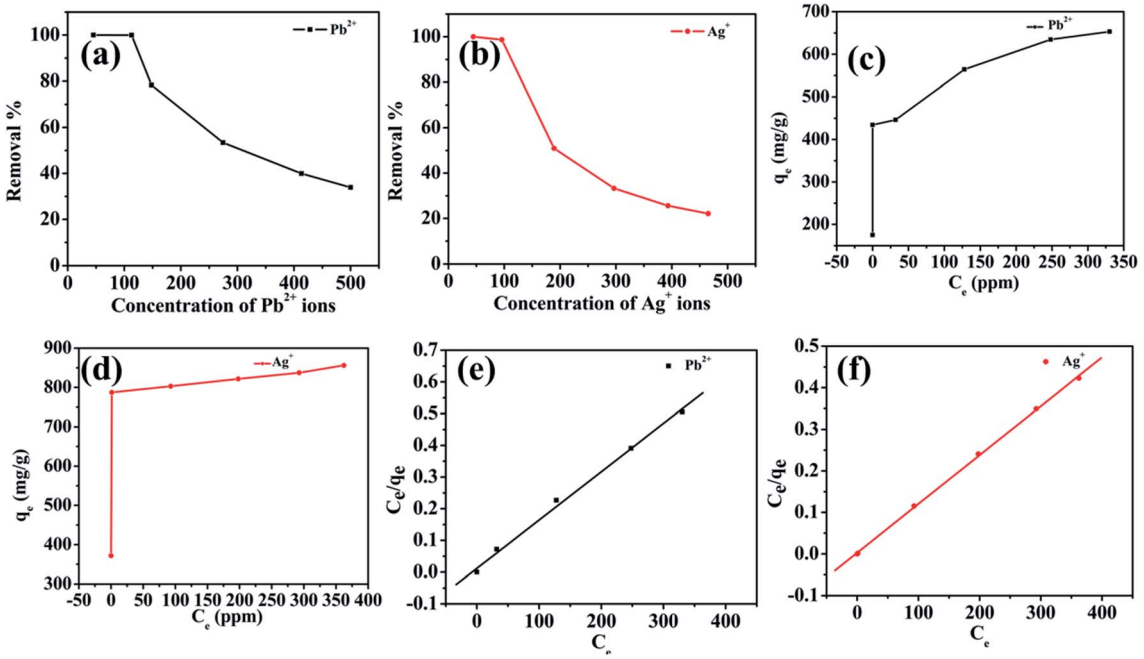

Fig. 8 Isotherm plots for Pb^{2+} and Ag^{+} removal: (a) removal% with respect to concentration variation of Pb^{2+} ions, (b) removal% with respect to concentration variation of Ag^{+} ions, (c) sorption isotherm for Pb^{2+} ions, (d) sorption isotherm for Ag^{+} ions, (e) Langmuir isotherm model for Pb^{2+} removal, (f) Langmuir isotherm model for Ag^{+} removal.

Table 4 Comparison of maximum adsorption capacities of MoS_4 LDH with different adsorbents

Adsorbents	Adsorbates	q_{max} (mg g^{-1})	References
Magnetic cellulose xanthate	Ag^+	166	45
S_4-LDH	Ag^+	383	46
Mg/Al–MoS_4-LDH	Ag^+	450	42
KMS-2	Ag^+	408	49
Ni/Fe/Ti–MoS_4-LDH	Ag^+	856	Present study
Mg/Al–MoS_4-LDH	Pb^{2+}	290	42
DTPA-LDH	Pb^{2+}	170	47
MNP–CTS	Pb^{2+}	140	48
Ni/Fe/Ti–MoS_4-LDH	Pb^{2+}	653	Present study

Table 5 Langmuir and Freudlich parameters

	Langmuir model			Freundlich model		
Adsorbates	q_m (mg g^{-1})	b (L mg^{-1})	R^2	K_f (mg g^{-1}) (L mg^{-1})$^{1/n}$	$1/n$	R^2
Pb^{2+}	654	0.134	0.998	490.90	0.032	0.76
Ag^+	848	0.011	0.999	616.59	0.06	0.93

uniform distribution of heat occurred over a heterogeneous surface and is represented as:

$$\log q_e = \log K_f + \frac{1}{n}\log C_e \quad (7)$$

where q_e and C_e have their usual meanings, and K_f and n denote Freundlich constants. These constants are obtained from the intercept and slope of a linear plot between log q_e and log C_e. The linear Freundlich fitting is illustrated in Fig. 9, and the parameters are clubbed in Table 5. From the summarized data in Table 5, it can be claimed that the Langmuir model was in high correlation for both the metal ions. Hence, it could be stated that the metal adsorption is a monolayer.

3.5 Adsorbent stability after heavy metal ion adsorption

After the sorption study, the adsorbent was recollected using the centrifugation technique, and the stability of MoS_4-LDH and adsorption were analyzed by FTIR spectroscopy (depicted in Fig. 10). The band which occurred at 1360 cm^{-1} in the spectrum of NO_3-LDH, which is the characteristic band of nitrate ion was absent in all the six samples after metal ion adsorption, which indicates that no NO_3^- ions accompanied the heavy metal ions during the adsorption process. The constant vibrations at 1628, 1422, 1233, and 1105 cm^{-1} imply the LDH stability during the sorption process.[42] Based on previously reported studies and the complexation chemistry of $(MoS_4)^{2-}$ ions, three mechanisms could be held responsible for such metal ion capture. The first mechanism is based on the condition when lower content of metal ions is present, and adsorbent is present in large concentration. Under such circumstance, the amount of active intercalated $(MoS_4)^{2-}$ sites are much higher than the metal ion (M^{n+}), and the excess $(MoS_4)^{2-}$ ions combine with M^{n+} resulting into the formation of complex moiety such as $[M(MoS_4)_2]^{2-}$ (when the charge on the metal ion is 2), which retains within the

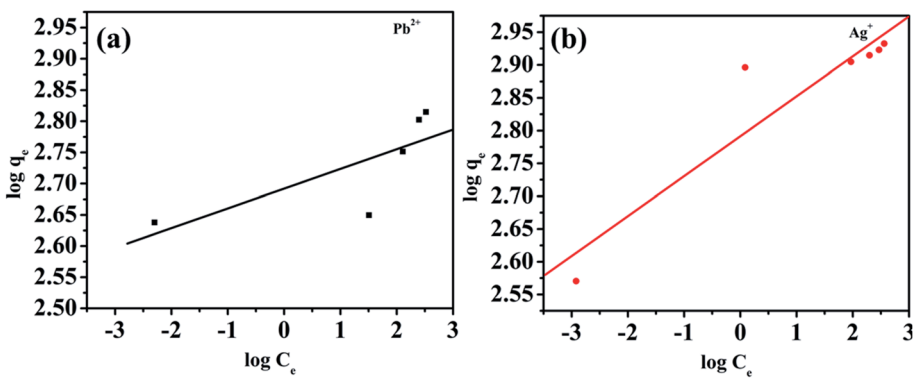

Fig. 9 (a) Freundlich isotherm model for Pb^{2+} removal, (b) Freundlich isotherm model for Ag^+ removal.

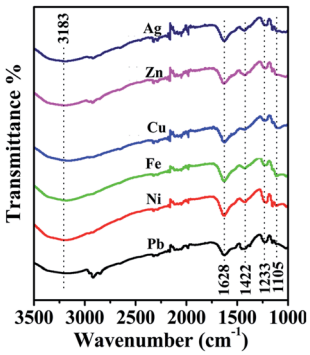

Fig. 10 FTIR spectra of MoS_4-LDH after metal ions adsorption.

LDH layers. The second mechanism occurs when both the ions are present in almost equal amounts. In such a case, $(MoS_4)^{2-}$ ions are still present in excess quantity compared to the M^{2+} ions, and $[M(MoS_4)_2]^{2-}$ complex is dominant with an almost equal amount of LDH-NO_3. The third mechanism occurs when the metal cations are present in excess amount and the LDH-$(MoS_4)^{2-}$ gets saturated with the coordinated metal ions. Hence, the formation of amorphous neutral salt occurs along with the intercalated nitrate phase.[42]

4. Conclusion

MoS_4-LDH follows ion-exchange chemistry, during the formation process by replacing the nitrate ions with $(MoS_4)^{2-}$ ions in the layer spacing of hydrothermally synthesized NiFeTi LDH. Due to the tremendous increase in pollution caused by heavy metals and the scarcity of available techniques, it has become essential to design an efficient adsorbent for heavy metals uptake. Sulfide groups present in the $(MoS_4)^{2-}$ ions show excellent uptake towards soft Lewis metal ions due to their soft Lewis basic properties. When all the heavy metal ions are present in aqueous solution, the material showed greater selectivity for Pb^{2+} and Ag^{+} ions ($Ni^{2+} < Cu^{2+} < Zn^{2+} < Fe^{3+} < Pb^{2+} < Ag^{+}$) and high adsorption capacities, 653 and 856 mg g^{-1}, for Pb^{2+} and Ag^{+} ions, respectively. The adsorption was found to obey the pseudo-second-order model towards Pb^{2+} and Ag^{+} ions supporting the chemisorption process *via* the formation of M–S bonding. All the above-mentioned features suggest ternary MoS_4-LDH material be very efficient for the removal of heavy metals from polluted water.

Conflicts of interest

The authors have no conflict regarding the publication of the paper.

Acknowledgements

GR and RC are highly thankful to the University of Delhi for providing financial support.

References

1 D. Howard, We have 10 years to save the seas, *Global Oceanic Environmental Survey*, September 1, 2019.
2 G. Salehi, R. Abazari and A. R. Mahjoub, Visible-Light-Induced Graphitic-C_3N_4@Nickel-Aluminum Layered Double Hydroxide Nanocomposites with Enhanced Photocatalytic Activity for Removal of Dyes in Water, *Inorg. Chem.*, 2018, **57**, 8681–8691.
3 D. Li, S. Zeng, M. He and A. Z. Gu, Water Disinfection Byproducts Induce Antibiotic Resistance-Role of Environmental Pollutants in Resistance Phenomena, *Environ. Sci. Technol.*, 2016, **50**, 3193–3201.
4 X. Gong, D. Huang, Y. Liu, G. Zeng, R. Wang, J. Wei, C. Huang, P. Xu, J. Wan and C. Zhang, Pyrolysis and reutilization of plant residues after phytoremediation of heavy metals contaminated sediments: for heavy metals stabilization and dye adsorption, *Bioresour. Technol.*, 2018, **253**, 64–71.
5 H. He, Z. Xiang, H. Chen, X. Chen, H. Huang, M. Wen and C. Yang, Biosorption of Cd(II) from synthetic wastewater using dry biofilms from biotrickling filters, *Int. J. Environ. Sci. Technol.*, 2018, **15**, 1491–1500.
6 O. Pourret and J. C. Bollinger, What to do now: to use or not to use?, *Sci. Total Environ.*, 2018, **610**, 419–420.
7 B. K. Bansod, T. Kumar, R. Thakur and S. Rana, A review on various electrochemical techniques for heavy metal ions detection with different sensing platforms, *Biosens. Bioelectron.*, 2017, **94**, 443–455.
8 X. Gong, D. Huang, Y. Liu, G. Zeng, R. Wang, J. Wan, C. Zhang, M. Cheng, X. Qin and W. Xue, Stabilized nanoscale zerovalent iron mediated cadmium accumulation and oxidative damage of Boehmeria nivea (L.) gaudich cultivated in cadmium contaminated sediments, *Environ. Sci. Technol.*, 2017, **51**, 11308–11316.
9 F. Fu and W. Qi, Removal of heavy metal ions from wastewaters: a review, *J. Environ. Manag.*, 2011, **92**, 407–418.
10 G. Liu, X. Chai, Y. Shao, L. Hu, Q. Xie and H. Wu, Toxicity of copper, lead, and cadmium on the motility of two marine microalgae Isochrysis galbana and Tetraselmis chui, *J. Environ. Sci.*, 2011, **23**, 330–335.
11 Ö. Gerçel and H. F. Gerçel, Adsorption of lead(II) ions from aqueous solutions by activated carbon prepared from biomass plant material of Euphorbia rigida, *Chem. Eng. J.*, 2007, **132**, 289–297.
12 M. Momčilović, M. Purenović, A. Bojić, A. Zarubica and M. Ranđelović, Removal of lead(II) ions from aqueous solutions by adsorption onto pine cone activated carbon, *Desalination*, 2011, **276**, 53–59.
13 N. Muhammad, N. Banooria, A. Akbarb, A. Azizullah, M. Khan, M. Qasim and H. Rahman, Microbial and toxic metal contamination in well drinking water: potential health risk in selected areas of Kohat, Pakistan, *Urban Water J.*, 2017, **14**, 394–400.

14 Z. Xia, L. Baird, N. Zimmerman and M. Yeager, Heavy metal ion removal by thiol functionalized aluminum oxide hydroxide nanowhiskers, *Appl. Surf. Sci.*, 2017, **416**, 565–573.
15 M. Nemati, S. M. Hosseini and M. Shabanian, Novel electrodialysis cation exchange membrane prepared by 2-acrylamido-2-methylpropane sulfonic acid; heavy metal ions, *J. Hazard. Mater.*, 2017, **337**, 90–104.
16 G. G. Aregay, A. Jawad, Y. Du, A. Shahzad and Z. Chen, Efficient and selective removal of chromium(VI) by sulfide assembled hydrotalcite compounds through concurrent reduction and adsorption processes, *J. Mol. Liq.*, 2019, **294**, 111532.
17 T. K. Tran, K. F. Chiu, C. Y. Lin and H. J. Leu, Electrochemical treatment of wastewater: selectivity of the heavy metals removal process, *Int. J. Hydrogen Energy*, 2017, **10**, 27741–27748.
18 J. Guo, Y. Kang and Y. Feng, Bioassessment of heavy metal toxicity and enhancement of heavy metal removal by sulfate-reducing bacteria in the presence of zero valent iron, *J. Environ. Manage.*, 2017, **203**, 278–285.
19 R. Kumar, G. B. V. S. Lakshmi, K. Singh and P. R. Solanki, A novel approach towards optical detection and detoxification of Cr(VI) to Cr(III) using L-Cys-VS_2QDs, *J. Environ. Chem. Eng.*, 2019, **7**, 103202.
20 N. Chaudhary, P. K. Gupta, S. Eremin and P. R. Solanki, One-step green approach to synthesize highly fluorescent carbon quantum dots from banana juice for selective detection of copper ions, *J. Environ. Chem. Eng.*, 2020, **8**, 103720.
21 S. Verma and R. K. Dutta, Development of cysteine amide reduced graphene oxide (CARGO) nano-adsorbents for enhanced uranyl ions removal from aqueous medium, *J. Environ. Chem. Eng.*, 2017, **5**, 4547–4558.
22 X. H. Wang, W. Y. Deng, Y. Y. Xie and C. Y. Wang, Selective removal of mercury ions using a chitosan–poly(vinyl alcohol) hydrogel adsorbent with three-dimensional network structure, *Chem. Eng. J.*, 2013, **228**, 232–242.
23 G. Blanchard, M. Maunaye and G. Martin, Removal of heavy metals from waters by means of natural zeolites, *Water Res.*, 1984, **18**(12), 1501–1507.
24 D. Mohan and P. S. Kunwar, Single-and multi-component adsorption of cadmium and zinc using activated carbon derived from bagasse—an agricultural waste, *Water Res.*, 2002, **36**, 2304–2318.
25 X. Zhao, Q. Jia, N. Song, W. Zhou and Y. Li, Adsorption of Pb(II) from an aqueous solution by titanium dioxide/carbon nanotube nanocomposites: kinetics, thermodynamics, and isotherms, *J. Chem. Eng. Data*, 2010, **55**, 4428–4433.
26 W. Du, L. Yin, Y. Zhuo, Q. Xu, L. Zhang and C. Chen, Catalytic oxidation and adsorption of elemental mercury over $CuCl_2$-impregnated sorbents, *Ind. Eng. Chem. Res.*, 2014, **53**, 582–591.
27 J. Liu, Y. Ma, T. Xu and G. Shao, Preparation of zwitterionic hybrid polymer and its application for the removal of heavy metal ions from water, *J. Hazard. Mater.*, 2010, **178**, 1021–1029.
28 A. B. Albadarin, H. Ala'a, N. A. Al-Laqtah, G. M. Walker, S. J. Allen and M. N. M. Ahmad, Biosorption of toxic chromium from aqueous phase by lignin: mechanism, effect of other metal ions and salts, *Chem. Eng. J.*, 2011, **169**, 20–30.
29 V. Tharanitharan and K. Srinivasan, Kinetic and equilibrium studies of removal of pb(ii) and cd(ii) ions from aqueous solution by modified duolite XAD-761 resins, *Asian J. Chem.*, 2010, **22**, 3036.
30 A. Benhammou, A. Yaacoubi, L. Nibou and B. Tanouti, Adsorption of metal ions onto Moroccan stevensite: kinetic and isotherm studies, *J. Colloid Interface Sci.*, 2005, **282**, 320–326.
31 A. I. Khan and D. O'Hare, Intercalation chemistry of layered double hydroxides: recent developments and applications, *J. Mater. Chem.*, 2002, **12**, 3191–3198.
32 V. R. L. Constantino and T. J. Pinnavaia, Structure-reactivity relationships for basic catalysts derived from a $Mg^{2+}/A1^{3+}/CO_3^-$ layered double hydroxide, *Catal. Lett.*, 1994, **23**(3–4), 361–367.
33 A. Corma, V. Fornes, F. Rey, A. Cervilla, E. Llopis and A. Ribera, Catalytic air oxidation of thiols mediated at a Mo(VI) O_2 complex center intercalated in a Zn(II)-Al(III) layered double hydroxide host, *J. Catal.*, 1995, **152**, 237–242.
34 G. Rathee, N. Singh and R. Chandra, Simultaneous Elimination of Dyes and Antibiotic with a Hydrothermally Generated NiAlTi Layered Double Hydroxide Adsorbent, *ACS Omega*, 2020, **5**(5), 2368–2377.
35 V. Rives and M. A. Ulibarri, Layered double hydroxides (LDH) intercalated with metal coordination compounds and oxometalates, *Coord. Chem. Rev.*, 1999, **181**, 61–120.
36 X. Xue, Q. Gu, G. Pan, J. Liang, G. Huang, G. Sun, S. Ma and X. Yang, Nanocage structure derived from sulfonated β-cyclodextrin intercalated layered double hydroxides and selective adsorption for phenol compounds, *Inorg. Chem.*, 2014, **53**, 1521–1529.
37 A. C. Sutorik and M. G. Kanatzidis, Stabilization of uranyl cations in molten sodium polysulfide and formation of the novel solid oxysulfide $Na_4(UO_2)Cu_2S_4$, *J. Am. Chem. Soc.*, 1997, **119**(33), 7901–7902.
38 A. Müller, E. Krickemeyer, V. Wittneben, H. Bögge and M. Lemke, $(NH_4)_2[Re_2S_{16}]$, a soluble metal sulfide with interesting electronic properties and unusual reactivity, *Angew. Chem., Int. Ed. Engl.*, 1991, **30**, 1512–1514.
39 G. Rathee, A. Awasthi, D. Sood, R. Tomar, V. Tomar and R. Chandra, A new biocompatible ternary layered double hydroxide adsorbent for ultrafast removal of anionic organic dyes, *Sci. Rep.*, 2019, **9**, 1–14.
40 S. Ma, C. Fan, L. Du, G. Huang, X. Yang, W. Tang, Y. Makita and K. Ooi, Intercalation of macrocyclic crown ether into well-crystallized LDH: formation of staging structure and secondary host–guest reaction, *Chem. Mater.*, 2009, **21**, 3602–3610.
41 M. J. Manos, N. Ding and M. G. Kanatzidis, Layered metal sulfides: exceptionally selective agents for radioactive strontium removal, *Proc. Natl. Acad. Sci. U. S. A.*, 2008, **105**(10), 3696–3699.

42 L. Ma, Q. Wang, S. M. Islam, Y. Liu, S. Ma and M. G. Kanatzidis, Highly selective and efficient removal of heavy metals by layered double hydroxide intercalated with the MoS_4^{2-} ion, *J. Am. Chem. Soc.*, 2016, **138**, 2858–2866.

43 K. Gupta, J. B. Huo, J. C. E. Yang, M. L. Fu, B. Yuan and Z. Chen, $(MoS_4)^{2-}$ intercalated $CAMoS_4$·LDH material for the efficient and facile sequestration of antibiotics from aqueous solution, *Chem. Eng. J.*, 2019, **355**, 637–649.

44 J. Ali, Z. Liao, Z. Zhou, A. Khan, T. Wang, J. Ifthikar, A. Shahzad, Z. Chen and Z. Chen, Fe-MoS_4: an effective and stable LDH-based adsorbent for selective removal of heavy metals, *ACS Appl. Mater. Interfaces*, 2017, **9**, 28451–28463.

45 M. H. Beyki, M. Bayat, S. Miri, F. Shemirani and H. Alijani, Synthesis, characterization, and silver adsorption property of magnetic cellulose xanthate from acidic solution: prepared by one step and biogenic approach, *Ind. Eng. Chem. Res.*, 2014, **53**, 14904–14912.

46 S. Ma, Q. Chen, H. Li, P. Wang, S. M. Islam, Q. Gu, X. Yang and M. G. Kanatzidis, Highly selective and efficient heavy metal capture with polysulfide intercalated layered double hydroxides, *J. Mater. Chem.*, 2014, **2**, 10280–10289.

47 X. Liang, W. Hou, Y. Xu, G. Sun, L. Wang, Y. Sun and X. Qin, Sorption of lead ion by layered double hydroxide intercalated with diethylenetriaminepentaacetic acid, *Colloids Surf., A*, 2010, **366**, 50–57.

48 L. Zhou, L. Ji, P. C. Ma, Y. Shao, H. Zhang, W. Gao and Y. Li, Development of carbon nanotubes/$CoFe_2O_4$ magnetic hybrid material for removal of tetrabromobisphenol A and Pb(II), *J. Hazard. Mater.*, 2014, **265**, 104–114.

49 Z. H. Fard, C. D. Malliakas, J. L. Mertz and M. G. Kanatzidis, Direct extraction of Ag^+ and Hg^{2+} from cyanide complexes and mode of binding by the layered $K_2MgSn_2S_6$ (KMS-2), *Chem. Mater.*, 2015, **27**, 1925–1928.

50 J. P. Simonin, On the comparison of pseudo-first order and pseudo-second order rate laws in the modeling of adsorption kinetics, *Chem. Eng. J.*, 2016, **300**, 254–263.

51 A. Jawad, L. Peng, Z. Liao, Z. Zhou, A. Shahzad, J. Ifthikar, M. Zhao, Z. Chen and Z. Chen, Selective removal of heavy metals by hydrotalcites as adsorbents in diverse wastewater: different intercalated anions with different mechanisms, *J. Cleaner Prod.*, 2019, **211**, 1112–1126.